

Oily sludge catalytic pyrolysis combined with fine particle removal using a Ni-ceramic membrane

Ningbo Gao ^{1*}, Jiaqi Li ¹, Cui Quan ¹, Xiao Wang ¹, Yang Yang ²

¹ School of Energy and Power Engineering, Xi'an Jiaotong University, Xi'an, 710049, China.

² Bioenergy Research Group, EBRI, Aston University, Birmingham B4 7ET, UK.

*Corresponding author: nbogao@xjtu.edu.cn

Abstract

Pyrolysis is one of the effective technology for oily sludge treatment and energy recovery. However, pyrolysis of oily sludge generates solid particles which are taken away from the reactor by gas, causing blockage in downstream equipment and reducing the quality of pyrolysis oil and gas. A study on the clean catalytic pyrolysis of oily sludge was carried out, by incorporating a ceramic membrane with or without Ni inside the pyrolysis reactor. It aims to investigate the effect of ceramic membrane on oily sludge pyrolysis and particulate removal. The yield of the pyrolysis gas produced from the reaction with Ni-ceramic membrane is 31.46 L/kg, while the recovery rate of pyrolysis oil is 48.21%. On the contrary, the yield of the pyrolysis gas produced from the reaction with blank ceramic membrane is 17.92 L/kg, while the recovery rate of pyrolysis oil is 62.63%. The particulate matter content in gas without and with Ni-ceramic membrane are 2.74 and 0.07 mg/L. The particulate matter content in oil without and with Ni-ceramic membrane are 3708.9 and 156.7 mg/L, respectively. Results indicated that the Ni catalyst loading on the ceramic membrane could improve the yield of the pyrolysis gas and remove the fine particles effectively. In addition, a long-time catalytic pyrolysis experiment was carried out, with the feeding speed of 4.17 g/min and the reaction temperature of 500 °C. It was found from the set conditions that the Ni-ceramic membrane could be

23 used continuously for 420 min.

24 **Key words:** Oily sludge; Catalytic pyrolysis; Ni-ceramic membrane; Particulate matter

25

26 **1. Introduction**

27 The operations of crude oil exploration, production, transportation, storage and refining can generate
28 a great deal of oily sludge in petroleum industry [1]. Oily sludge is a complex semi-solid mixture
29 which consists of water, various petroleum hydrocarbons, solid material and metals. Oily sludge is
30 considered as hazardous waste in many countries due to its hazardous nature [2]. The serious threats
31 to the environment and human health was posed with insufficient disposal or treatment of oily sludge
32 [3]. Therefore, the effective recovery and utilization method of oily sludge has attracted a growing
33 attention in recent years.

34 Pyrolysis is a method of thermal decomposition of organic materials at high temperature in an inert
35 environment [4]. The pyrolysis process of oily sludge produces solid product (chars), condensable
36 hydrocarbons (oil) and non-condensable gases. The recovered oil could be used as fuels or sources of
37 other valuable chemical products [5]. Furthermore, pyrolysis gas and char can be used to provide
38 heat and generate electricity [6]. Several studies have been reported to use pyrolysis for fuel recovery
39 from oily sludge. Qin et al [7] studied the pyrolysis of oily sludge in a fluidized bed reactor. The
40 results demonstrated that the maximum oil yield (59.20%) was achieved at 500 °C and the
41 simultaneous recovery of oil and iron from oily sludge by pyrolysis was feasible. Schmidt et al [8]
42 pointed out that about 70-84% of oil could be recycled from oily sludge during pyrolysis at a
43 temperature range of 460-650 °C in a fluidized bed reactor. The pyrolysis oil was close to the diesel
44 oil, however, abundant heavy components (such as asphaltene and gelatin) severely affect the quality
45 of oil products [9].

46 Pyrolysis of oily sludge generates solid fine particles which are removed from the reactor by carrier
47 gas. These particles can cause fouling and blockage of downstream equipment. Furthermore, the

48 quality of pyrolysis oil and gas are reduced and are not suitable to be used as alternative fuels due to
49 the existence of large number of solid particles in oil and gas. Therefore, it is necessary to find an
50 effective method to remove particles from oil and gas to obtain high quality products. However,
51 obstacles exist to restrict development of particle removal technology. The removal of particles from
52 oil and gas products respectively will increase the processing cost obviously. In addition, it is
53 difficult to remove particles from the pyrolysis oil under room temperature. To solve these problems,
54 a high temperature filtration unit can be used to reduce the particles from high temperature gas
55 before it condenses into oil. In this way, the particles in pyrolysis oil and pyrolysis gas can be
56 removed simultaneously.

57 Furthermore, useful catalysts were added during the pyrolysis process to improve the quality of oil
58 products. The catalytic cracking methods are feasible in lowering reaction temperature, shortening
59 reaction time and changing product distribution [10]. Vast amount of studies on the addition of
60 catalysts to the oily sludge during the pyrolysis process have been conducted. A variety of catalysts
61 have been widely used for the oily sludge pyrolysis, such as aluminum compounds (Al, Al₂O₃ and
62 AlCl₃), iron compounds (Fe, Fe₂O₃, FeCl₃ and FeSO₄·7H₂O), calcium compounds (CaO, Ca(OH)₂,
63 CaCl₂ and CaCO₃), Ni-based catalysts, Co-based catalysts, KOH, dolomite and olivine [11-15]. Lin
64 et al [11] suggested that quality of pyrolysis oil was improved due to the addition of KOH according
65 to smaller average molecular weight, lower viscosity, higher heating value, less asphaltenes and more
66 straight chain hydrocarbons.

67 Nowadays, the research focus in pyrolysis of oily sludge is to develop new catalyst with high
68 performance. Ni-based catalysts have shown an excellent advantage in the pyrolysis and gasification
69 reaction, with an activity comparable to noble metal catalysts [16-18]. The catalytic activity is related

70 to the carriers' property, active phase precursor, synthesis and pretreatment method [19, 20]. The
71 supporting material is considered as the key role in the performance of the Ni-based catalyst.
72 Ceramic membrane is a porous material with high porosity. Ceramic membranes have some
73 advantages such as high chemical, mechanical, thermal resistance and low price [21, 22]. Due to the
74 good physical properties of ceramic membrane, it can be used as Ni-based catalyst carrier for oily
75 sludge pyrolysis to improve the quality of products. So far, there are few studies on the ceramic
76 membrane as active core to support nickel for oily sludge pyrolysis.

77 Furthermore, our previous research results suggested that the ceramic membrane can remove
78 particulate matter from the pyrolysis gas [23]. In order to improve the quality of pyrolysis products
79 and remove particulate matter at the same time, tubular ceramic membrane was selected as the
80 catalyst carrier. Therefore, the Ni-ceramic membrane catalyst was prepared in this study. Moreover,
81 the clean catalytic pyrolysis of oil sludge was carried out by incorporating a tubular ceramic
82 membrane inside the pyrolysis reactor for the pyrolysis of oily sludge, aiming to significantly
83 enhance the removal of particles from the pyrolysis gas and the improvement of product quality.

84 **2. Experimental section**

85 **2.1 Materials**

86 The oily sludge was selected as raw material from Shaanxi Yanchang Petroleum Group in China.
87 Proximate analysis was performed with a muffle furnace (Yamato FO410C, Japan) according to the
88 standard method (GB/T 212-2008). C, H, N and S analysis of oily sludge was obtained with an
89 Elementar Vaeio MACRO elemental analyzer. The estimation content of O is carried out by
90 subtracting the sum of other compositions (ash, C, H, N and S) from 100%. Table 1 shows the
91 proximate and ultimate analysis results, oil content and HHV of oily sludge. The result indicates the

92 oily sludge of low moisture, moderate volatile matter, high ash and very low fixed carbon content.
 93 Soxhlet extraction was used to measure the oil content of oily sludge, which was 17.89%. The
 94 calorific value was measured with a bomb calorimeter (Sande SDC-5015, China) with 8.12 MJ /kg.

95 Table 1 Properties of oily sludge sample

Proximate analysis ^a (wt%)				Ultimate analysis ^b (wt%)					Oil content (wt%)	HHV (MJ/kg)
M	V	A	FC	C	H	O ^c	N	S		
10.64	21.03	65.27	3.06	70.13	11.85	8.72	3.43	5.87	17.89	8.12

96 ^a On received basis. ^b On ash-free basis. ^c By difference.

97 Thermogravimetric (TG) analysis was carried out using a thermogravimetric analyzer (Shimadzu
 98 TG-DSC STA449F3, Japan). Nitrogen was used as purge gas, and the flow rate was 75 ml/min.
 99 10-15 mg of oily sludge samples were heated from room temperature to 900 °C at heating rates of 5,
 100 10, 15 and 20 °C/min under nitrogen atmosphere to test the effect of heating rates on pyrolysis.

101 2.2 Catalyst preparation

102 Impregnation method was employed to prepare Ni-ceramic membrane (Ni-CM) catalyst. The
 103 specific amount of Ni(NO₃)₂·6H₂O was dissolved in deionized water to obtain 1 mol/L Ni(NO₃)₂
 104 solution. The clean ceramic membrane was dipped into the Ni(NO₃)₂ solution for 12h, and then the
 105 derived catalyst precursor was dried in an oven for 12h at 105 °C. The precursor was calcined under
 106 air atmosphere at 700 °C for 2h in a reactor, followed by reduction at 500 °C for 2h within mixture of
 107 nitrogen and hydrogen, for N₂/H₂ volume ratio of 4:1.

108 The total amount of Ni loading on Ni-ceramic membrane (Ni-CM) catalyst was calculated by using
 109 the following equation:

$$M_{CM} = \frac{M_{CM-1} - M_{CM-0}}{M_{CM-0}} \times 100\% \quad (1)$$

where, M_{CM} is the total amount of Ni loading on catalyst; M_{CM-1} is the weight of Ni-ceramic membrane catalyst, g; M_{CM-0} is the weight of clean ceramic membrane, g.

The total amount of Ni loading on each Ni-CM catalyst was controlled to be around 1.03%.

2.3 Catalyst characterization

Scanning electron microscopy and backscattered electron imaging (SEM/BSE, JEOL 7800F, Japan) were carry out to detect the microstructure of blank ceramic membrane, fresh Ni-CM and used Ni-CM catalyst, and distribution of different elements. Energy dispersive spectrometer (EDS) was used to measure content of the surface components. The association of catalysts was performed by using X-ray diffractometer (XRD, PANalytical XPertPRO, Netherlands). The range of 2 theta angle was changed from 10 to 95° with a scanning step of 4°/min. The X-ray fluorescence spectrometer (XRF, PANalytical Axios PW4400, Netherlands) was used to determine the elements of catalysts.

2.4 Experimental

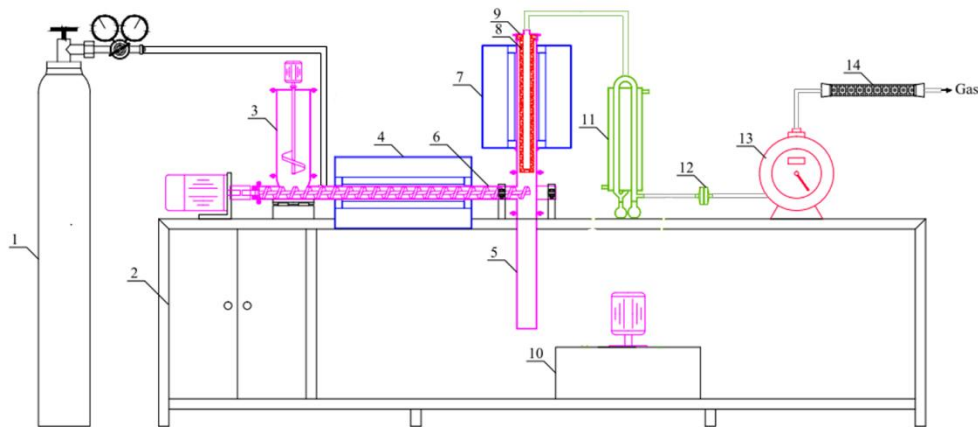


Figure 1. Schematic of oily sludge spiral pyrolysis apparatus

1. Nitrogen cylinder; 2. Control cabinet; 3. Feeding bin; 4. Tubular furnace A; 5. Residue collector; 6. Pyrolysis reactor; 7. Tubular furnace B; 8. Ceramic membrane; 9. Catalytic filter reactor; 10.

127 Cooling water; 11. Condenser; 12. Gas particle filter; 13. Wet gas meter; 14. Desiccator

128 The clean pyrolysis of oily sludge was carried out in a self-fabricated spiral continuous reactor,
129 which is shown in Figure 1. This device consists of a pyrolysis reactor with a spiral screw, a catalytic
130 filter reactor with a blank CM or a Ni-CM, an electrical heating system, a residue collector, a
131 condensing system and a gas product collection system. The temperatures of pyrolysis reactor,
132 catalytic filter reactor and residue collector were controlled by temperature regulator and K-type
133 thermocouples.

134 The oily sludge was placed in the feeding bin before each experiment. Then, N₂ with the flow rate of
135 200 mL/min was injected into the reactor to ensure an oxygen-free system. When the reactor
136 temperature reached the required value (500 °C), the oily sludge was fed to the reactor at a desired
137 feeding rate. The volatiles were fed into the catalytic filter reactor that fixes a Ni-CM catalyst. When
138 volatiles went through the Ni-CM catalyst, particulate matter entrained into the volatiles can be
139 trapped by the Ni-CM. The gas was reformed in the catalytic filter reactor and introduced to the
140 condensing system. The liquid product was separated and collected in a liquid tank. Meanwhile, gas
141 product passed through the gas particle filter, and the volume of gas was confirmed by a wet
142 flowmeter and dried by passing through a silica-gel drier. The pyrolysis gas was collected by a gas
143 collection bag. The numerical difference of wet flowmeter is the volume of pyrolysis gas generated
144 during the pyrolysis process. The pyrolysis residue was collected by residue collector and weighed
145 after the spiral pyrolysis apparatus cooled to room temperature. All experiments were repeated 3
146 times to obtain the accurate experimental data.

147 To evaluate the removal effect of ceramic membrane on particulate matter and catalytic effect of
148 Ni-CM on oily sludge pyrolysis, three contrast experiments with no CM (E1), blank CM (E2) and

149 Ni-CM catalyst (E3) in the catalytic filter reactor were performed at same operational conditions (i.e.
150 temperature of 500 °C, feeding speed of 4.17 g/min and reaction time of 2h).

151 **2.5 Product analyses**

152 **2.5.1 Pyrolysis oil and gas analyses**

153 The composition of the gas was analyzed off-line by a China Tianmei 7900 gas chromatograph (GC)
154 with a flame ionization detector (FID) and a thermal conductivity detector (TCD). Nitrogen was used
155 as a tracer of GC to quantify the volume percent of each gas product. The yields of oil and char were
156 estimated based on the weight of each product.

157 The high heating value (HHV) of oils was conducted by a bomb calorimeter (Sande SDC 501,
158 China). Furthermore, the composition analysis of oil products was conducted with a gas
159 chromatography-mass spectrometer (GC-MS, Agilent 7000B).

160 The output per unit, yield of pyrolysis products and the recovery rate of pyrolysis oil were calculated
161 according to the following equations:

$$162 \quad P_i = \frac{M_i}{M_{OS}} \quad (2)$$

$$163 \quad Y_i = \frac{P_i}{1000} \times 100\% \quad (3)$$

$$164 \quad R_{oil} = \frac{Y_{oil}}{C_{oil}} \times 100\% \quad (4)$$

165 where, P_i is the output per unit of pyrolysis products, g/kg; M_i is the volume of pyrolysis products, g;
166 M_{OS} is the mass of oily sludge, kg; Y_i is the yield of pyrolysis products; i represents the char, gas and
167 oil; R_{oil} is the recovery rate of pyrolysis oil; Y_{oil} is the yield of pyrolysis oil; C_{oil} is the oil content of
168 oily sludge.

169 **2.5.2 Particulate matter analyses**

170 After the end of the experiment, the gas filtration membrane was taken out of the gas particle filter.
171 Furthermore, pyrolysis oil was passed through the oil filtration membrane. After that, the oil and gas
172 filtration membrane were rinsed with CH₂Cl₂ continuously until the filtrate was clarified. The oil and
173 gas filtration membrane were dried in the oven at 105 °C and weighed after cooling. The weight of
174 particles in the pyrolysis gas or oil is weight difference before and after use of gas or oil filter
175 membrane.

176 The content of particulate matter in pyrolysis gas can be expressed as:

$$177 \quad C_{gas-PM} = \frac{M_{gas-PM}}{V_{gas}} \quad (5)$$

178 where, C_{gas-PM} is the content of particulate matter in pyrolysis gas, mg/L; M_{gas-PM} is the mass of
179 particulate matter on the gas filtration membrane, mg; V_{gas} is the volume of the pyrolysis gas, L.

180 The content of particulate matter in pyrolysis oil can be expressed as:

$$181 \quad C_{oil-PM} = \frac{M_{oil-PM}}{V_{oil}} \quad (6)$$

182 where, C_{oil-PM} is the content of particulate matter in pyrolysis oil, mg/kg; M_{oil-PM} is the mass of
183 particulate matter on the oil filtration membrane, mg; V_{oil} is the volume of the pyrolysis oil, L.

184 The analysis of particle size and surface morphology of particulate matter was done by SEM. The
185 XRF (Axios PW4400, Holland) was used to measure the elemental composition of particulate matter.

186 **3. Results and Discussion**

187 **3.1 TG analysis of oily sludge pyrolysis**

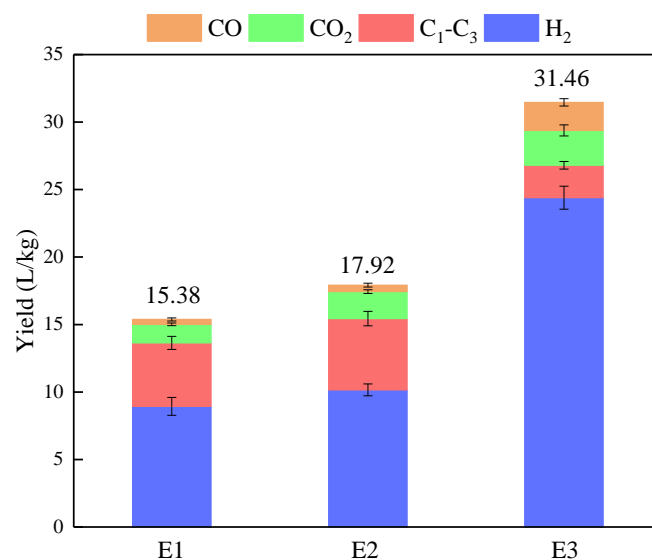
188 TG and DTG curves are the change curve of oily sludge mass and oily sludge weight loss rate with
189 temperature, respectively. Figure S1 shows the TG and DTG curves of oily sludge pyrolysis at
190 different heating rates. TG and DTG curves show similar trends at different heating rates. The DTG

191 curves are shifted towards the high temperature region with the increase of heating rate from 5 to
192 20 °C/min. Furthermore, the peak value of DTG curve increases with the increase of the heating rate.
193 The reason is that the high heating rate leads to the increase of the pyrolysis rate of oily sludge.
194 The pyrolysis process can be divided into three regions according to the DTG curves. In the first
195 region (from room temperature to 105 °C), 4.88-5.80 wt% of original weight is lost. It can be
196 expected that the weight loss is due to the evaporation of water. The most abundant release of
197 volatile matter (H₂, CO, CO₂, alkanes, alkenes and aromatic hydrocarbon) is observed in the
198 temperature range 105-550 °C, which is related to volatilization and decomposition of complex
199 organic components [24, 25]. The last weight loss (550-780°C) is attributed to the decomposition of
200 organic residues and inorganic matter such as heavy metal salts [26].
201 The activation energy of oily sludge pyrolysis is presented in Table S1. Coats-Redfern integral
202 method is used to calculate the activation energy (*E*) of oily sludge pyrolysis. The activation energy
203 of different heating rate has little difference, and increases with the increase of temperature. It can be
204 known from Table S1 that the activation energies of three temperature ranges of oily sludge pyrolysis
205 are 5.42-7.45, 16.09-22.03 and 35.17-68.54 kJ/mol, respectively.

206 **3.2 Influence of the Ni-CM on gas production**

207 The yield of each component in pyrolysis gas, and gas yield in E1 (with no CM), E2 (with blank CM)
208 and E3 (with Ni-CM) are shown in Figure 2. Compared with the blank experiment E1, the pyrolysis
209 gas yield of E2 increased slightly, and the distribution of H₂, CO, CO₂ and C₁~C₃ is similar to gas
210 component of E1. The residence time of pyrolysis gas prolonged after the ceramic membrane was
211 placed in the catalytic filter reactor, thus improving the gas reforming effect. Moreover, the blank
212 ceramic membrane had a little catalytic activity for pyrolysis gas reforming. The existence of few

213 active components (i.e. Fe_2O_3 , NiO) can strengthen the reforming of pyrolysis gas.
214 The yield of pyrolysis gas is 31.46 L/kg in the E3. The total volume of gas product and H_2
215 concentration are significantly enhanced due to the effect of Ni-CM catalyst. The total volume of gas
216 with Ni-CM catalyst increases to almost 2 times of the other tests (E1 and E2). Compared with pure
217 CM (E2), the H_2 yield increased from 10.16 to 24.40 L/kg with Ni-CM catalyst (E3). In addition, the
218 $\text{C}_1\text{-C}_3$ yield decreased significantly due to the high catalytic activity of Ni-CM catalyst on the
219 pyrolysis gas reforming. Ni catalyst can promote the fracture of C-C and C-H of macromolecular
220 long-chain aliphatic hydrocarbon in pyrolysis gas, and produce small molecular hydrocarbons such
221 as $\text{C}_1\text{-C}_3$ and H_2 [27, 28].
222 The lower heating value (LHV) of the pyrolysis gas in E1, E2 and E3 was calculated in this study.
223 The LHV of the pyrolysis gas in the E1, E2 and E3 is 23.53, 23.76 and 14.44 MJ/Nm^3 , respectively.
224 This phenomenon in the LHV can be ascribed to the high content $\text{C}_1\text{-C}_3$ of pyrolysis gas in E1 and
225 E2.

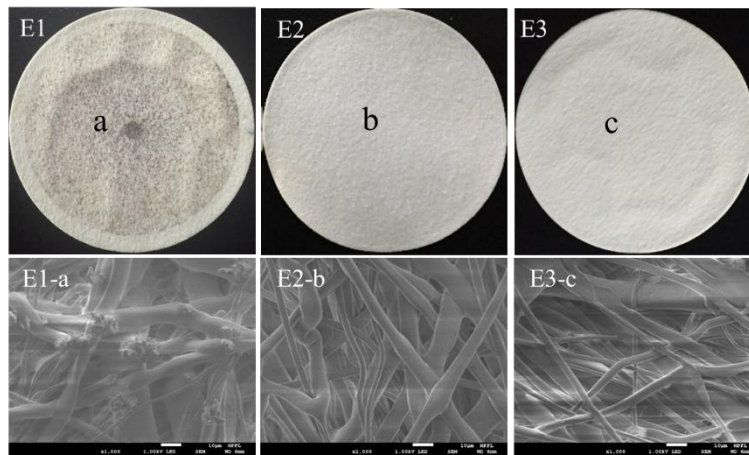


226

227

Figure 2. The yields of the pyrolysis gas, H_2 , CO , CO_2 and $\text{C}_1\text{-C}_3$

228 Figure 3 shows the appearance and SEM images of three gas filtration membranes of E1, E2 and E3,
 229 respectively. Three points a, b and c on the filter membranes were selected for SEM analysis. It can
 230 be found that more black particles deposited on E1 filtration filter membrane, which were produced
 231 without ceramic membrane. It can be seen from the SEM image that more amorphous particles
 232 deposited on the fibers of the E1 filter membrane. While there were no obvious solid particles
 233 depositing on E2 and E3 filter membrane. It might be attributed to the filtering effect of ceramic
 234 membranes in E2 and E3 test.



235
 236 Figure 3. The filtration membrane for particles in pyrolysis gas and the SEM image
 237 The particulate matter content of the pyrolysis gas is listed in Table 2. The particulate matter content
 238 in E1, E2 and E3 are 2.74 ± 0.29 , 0.17 ± 0.05 and 0.07 ± 0.02 mg/L, respectively. It can be known
 239 that ceramic membrane has an effective filtering effect on particulate matter in gas. The main
 240 elements of particulate matter were Si, Ca, Al, Mg, Na etc (as shown in Table S2).

241 Table 2 The particulate matter content of the pyrolysis gas

	E1	E2	E3
C_{gas-PM} (mg/L)	2.74 ± 0.29	0.17 ± 0.05	0.07 ± 0.02

242

243 **3.3 Influence of the Ni-CM on oil production**

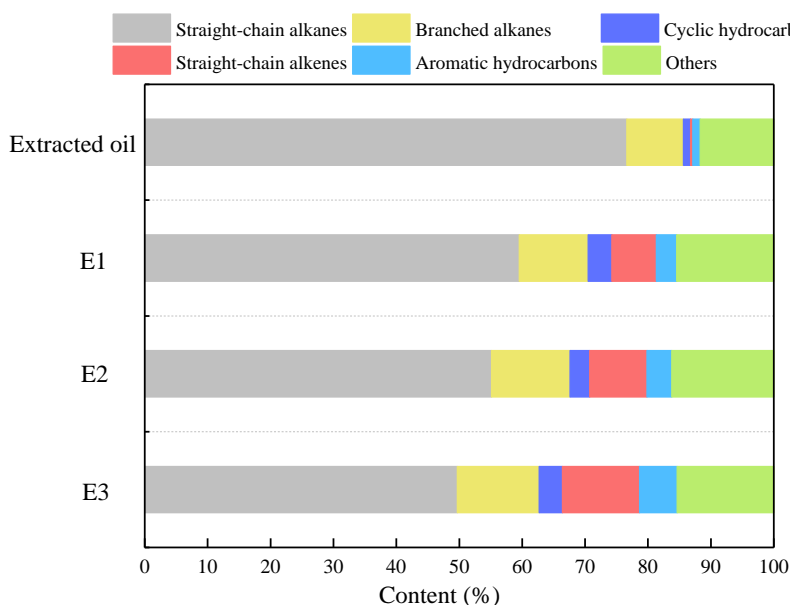
244 The unit yield, recovery rate and HHV of the oil produced in the E1, E2 and E3 are summarized in
 245 the Table 3. The oil recovery rate of E1, E2 and E3 are 72.50 ± 1.86 , 62.63 ± 0.85 and $48.21 \pm 1.27\%$,
 246 respectively. It means that the Ni-CM catalyst can well promoted thermal cracking of sample in the
 247 E3 experiment. The secondary reaction of degassing is converted into hydrogen with a smaller
 248 molecular weight and non-condensable, and C₁-C₃. The HHV of E2 and E3 oil are 37.14 and 37.78
 249 MJ/kg, respectively. The HHV of E1 oil is lowest due to the existence of solid particles.

250 Table 3 The yield, recovery rate and HHV of pyrolysis oil

	Unit yield (g/kg)	Recovery rate (%)	HHV (MJ/kg)
E1	129.72 ± 3.35	72.50 ± 1.86	35.15
E2	112.04 ± 1.52	62.63 ± 0.85	37.14
E3	86.24 ± 2.26	48.21 ± 1.27	37.78

251 As for the chemical components, the oil was analyzed by the GC-MS. The main identified
 252 components of the extracted oil and the pyrolysis oils (E1, E2 and E3) are shown in Figure 4. The
 253 hydrocarbons in the oil could be divided into straight-chain alkanes, branched alkanes, cyclic
 254 hydrocarbons, straight-chain alkenes, aromatic hydrocarbons and others. The dominant ones of the
 255 extracted oil are straight-chain alkanes and branched alkanes while the rest are cyclic hydrocarbons,
 256 straight-chain alkenes and aromatic hydrocarbons in small proportion. It has been proven that the
 257 pyrolysis oils have higher composition of branched alkanes, cyclic hydrocarbons, straight-chain
 258 alkenes and aromatic hydrocarbons compounds compared to extracted oil. Straight-chain alkenes
 259 were converted into other products such as cyclic hydrocarbons, straight-chain alkanes and aromatic
 260 hydrocarbons by chain breaking, dehydrogenation and isomerization during the pyrolysis process [29,
 261 30]. The contents of branched alkanes, cyclic hydrocarbons, straight-chain alkenes, aromatic

262 hydrocarbons of E1 oil is lower than that of E2 oil. It has been proven that the ceramic membrane
263 plays an important role to promote oily sludge pyrolysis reaction. The content of branched alkanes,
264 cyclic hydrocarbons, straight-chain alkenes and aromatic hydrocarbons in E3 is higher than that in
265 E2, which indicates that the nickel catalyst can promote the conversion of alkanes [31].

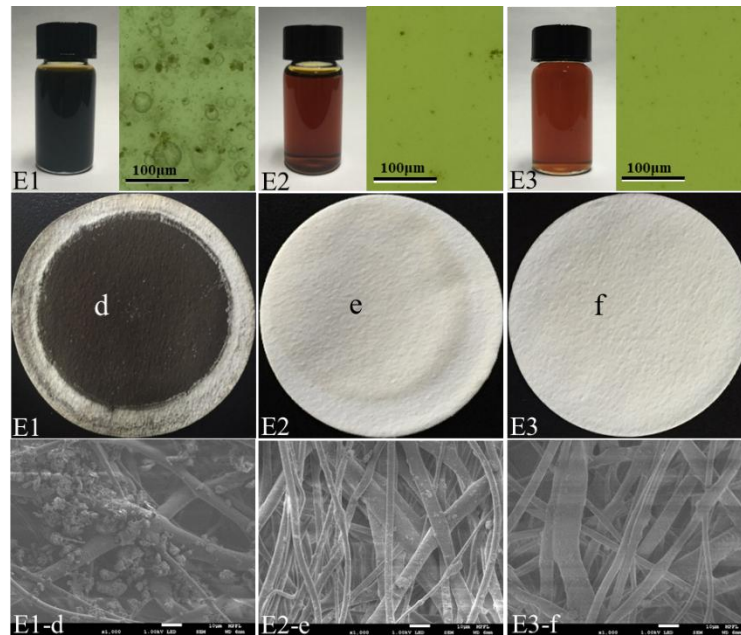


266

267 Figure 4. The analysis results of GC-MS of oil products

268 The oil of E1 (without CM), E2 (with blank CM) and E3 (with Ni-CM), and their high-magnification
269 micrographs are shown in Figure 5. The pyrolysis oil produced in E1 was black and turbid. It can be
270 seen from its high-magnification micrographs that some solid particles are mixed in the oil. The oil
271 of E2 and E3 are clear, transparent and brown, and there are no obvious particles in their
272 micrographs. The oil mixtures were filtered using 0.5 μ m pore size filter film to filter the particulate
273 matter. The appearance and SEM images of three filtration membranes of E1, E2 and E3 oil are also
274 presented in Figure 5. More black solid particles deposited on E1 filtration filter membrane, which
275 were produced without ceramic membrane. It can be seen that more amorphous solid particles
276 deposited on the fibers of the E1 filter membrane. While there are no obvious black solid particles

277 depositing on E2 and E3 filter membrane. It can be seen that a small layer of black solid particles is
278 trapped on the E1 filter, however, there are no obvious black solid particles on the E3 filter. Taking
279 SEM analysis of a, b and c points on the filter membrane, it can be found that many irregular solid
280 small particles are attached to the E1 filter fiber, the particles are adhered together, and there is
281 agglomeration. Furthermore, the E2 and E3 filter fibers are adhesion of some solid particles less than
282 5 μm on the other surface. It is further demonstrated that the ceramic membrane can effectively
283 retain solid particles having a particle size greater than 5 μm in the pyrolysis oil [32].



284

285 Figure 5. The images of oil samples and the particulate matter in oils

286 The particulate matter content of the pyrolysis oil is listed in Table 4. The particulate matter content
287 in E1, E2 and E3 are 3708.9 ± 90.3 , 234.6 ± 13.5 and 156.7 ± 8.2 mg/L, respectively. The results
288 indicate that the ceramic membrane has a great removal effect on solid particles. The XRF was used
289 to determine the element content of particulate matter (as shown in Table S3). The main elements of
290 particulate matter were Si, Ca, Al, Mg, Na etc, and amounts of trace heavy metal elements: Cr (978
291 mg/kg), Mn (929 mg/kg), Ni (495 mg/kg), Cu (143 mg/kg) and Zn (88 mg/kg).

292

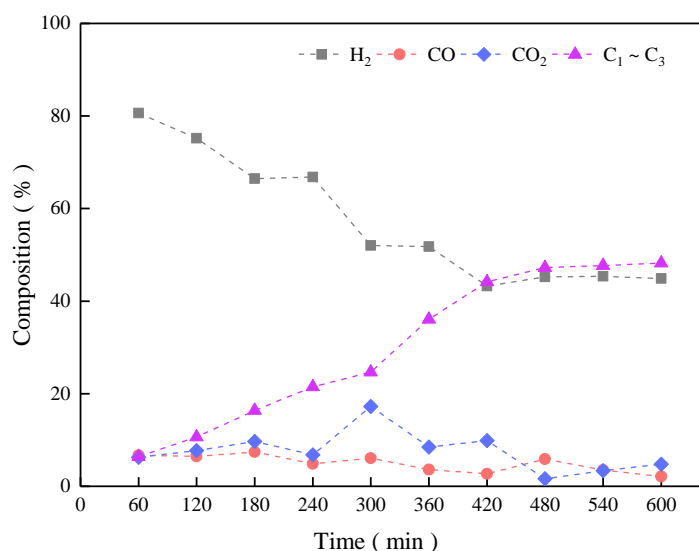
Table 4 The particulate matter content of pyrolysis oil

	E1	E2	E3
C_{oil-PM} (mg/L)	3708.9 ± 90.3	234.6 ± 13.5	156.7 ± 8.2

293

294 3.4 Life time analysis of catalyst

295 The stability of Ni-CM catalyst was tested during the long-time pyrolysis of oily sludge in the same
 296 reactor. The lifetime experiment (E4) was carried out at same experimental conditions (i.e. pyrolysis
 297 temperature of 500 °C and feeding rate of 4.17 g/min). Each gas bag was responsible for an hour to
 298 collect the pyrolysis gas. In Figure 6, it can be observed that the H₂ yield decreased from 80.16% to
 299 43.26% when the reaction time is below 420 min, while the content of C₁~C₃ increased from 6.42%
 300 at 60 min to 44.18% at 420 min. The content of H₂ and C₁~C₃ tend to be stable and fluctuated around
 301 45.00% when the reaction time was higher than 420 min. The content of CO was decreased during
 302 the whole pyrolysis process, while the CO₂ content fluctuated and remained at about 3.00% after 420
 303 min. The effective use time of Ni-CM catalyst was 420 min in the oily sludge catalytic pyrolysis
 304 experiment. With the increase of experimental time, coke deposits on the catalyst surface to decrease
 305 the catalytic activity.



306

307

Figure 6. Influence of reaction time on the composition of the pyrolysis gas

308

3.5 Characterizations of fresh and used catalysts

309

The SEM images of CM, fresh Ni-CM and used E4-Ni-CM with different magnification times of

310

1000 and 30000 are presented in Figure 7. It can be seen that the surface of blank CM is smooth, the

311

surface of fresh Ni-CM was covered by a layer of Ni particles, while more amorphous carbon

312

deposited on used E4-Ni-CM catalyst from the 1000-fold SEM images. It can be seen from the

313

30000-fold SEM image of fresh Ni-CM catalyst that Ni particle (<100 nm) is uniformly distributed

314

on the ceramic membrane's surface. In Figure 8, the surface of E4-Ni-CM is almost completely

315

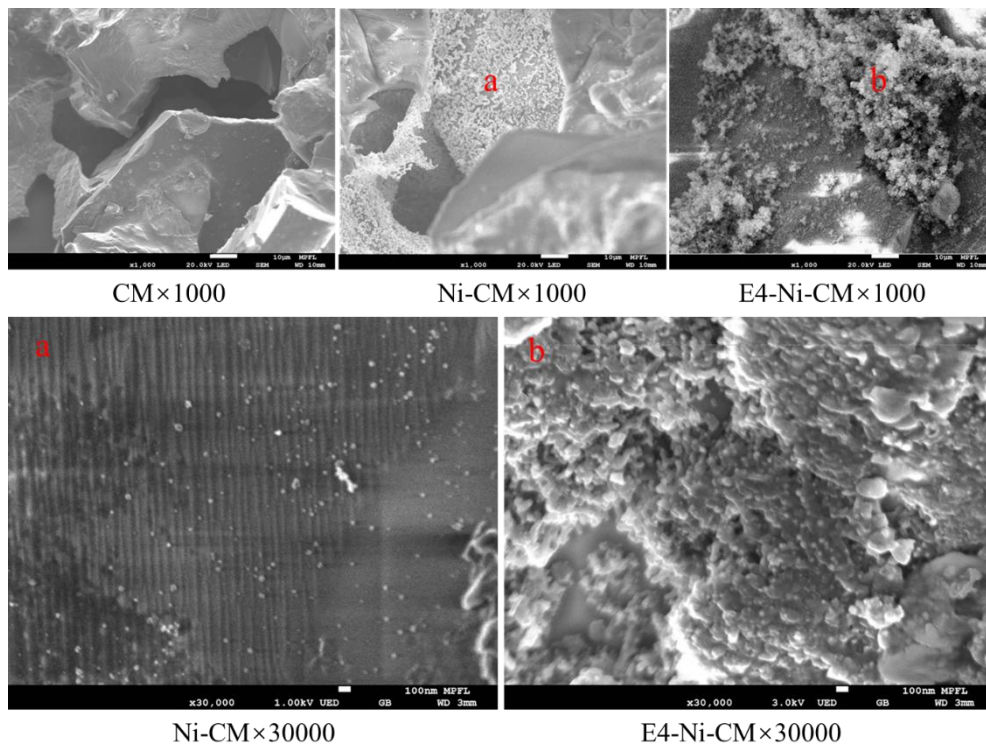
covered with carbon, and no Ni particles were observed on E4-Ni-CM catalyst. It is indicated that the

316

Ni-CM catalyst could not play its catalytic role and promote the secondary reforming of pyrolysis

317

gas.

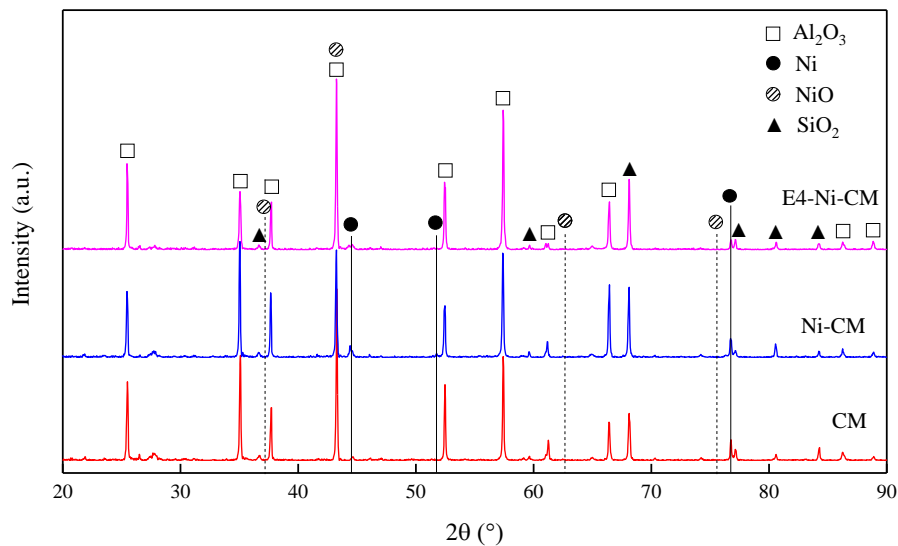


318
319 Figure 7. The SEM images of CM, Ni-CM, and E4-Ni-CM

320 BSE is an electron imaging technique based on SEM, which can reflect the element distribution on
 321 the sample surface. EDS technique is employed to show the Ni, Si and Al element distribution on the
 322 surface and inside of fresh catalyst. The SEM-BSE images with EDS mapping of surface and inside
 323 of fresh Ni-CM and used E4-Ni-CM were presented in Figure S2 and Figure S3, respectively. It can
 324 be seen that a large number of Ni particles are clustered in white spots on the BSE image. Mass of Ni
 325 particles are also scattered inside the fresh Ni-CM. For used catalyst shown in Figure S3, less
 326 aluminum indicates that the carbon completely deposited on the surface of ceramic membrane. A
 327 large amount of carbon was accumulated in the space inside E4-Ni-CM, and Ni particles were
 328 detected at the space of carbon accumulation, as shown in Figure S3.

329 XRF analysis results of blank CM, fresh Ni-CM catalyst and E4-Ni-CM catalyst are shown in Table
 330 S4. Based on the elemental composition, it is observed that both blank CM, fresh Ni-CM catalyst and
 331 E4-Ni-CM catalyst have a high content of Si (28%) and Al (>11%). Some metals such as Na, Ti, K,

332 Mg, Ca, Fe, Zr, Sr, Cr, and Mn are also detected in the ceramic membrane. The contents of nickel are
333 about 1.96% and 1.64% in the fresh Ni-CM and used E4-Ni-CM, respectively. This decrease of
334 nickel content is mainly due to the coverage of carbon on used E4-Ni-CM catalyst.



335

336 Figure 8. The XRD patterns of CM, Ni-CM, E4-Ni-CM.

337 Figure 8 presents the XRD patterns of blank CM, fresh Ni-CM and used E4-Ni-CM catalysts. Al_2O_3
338 is the main component of ceramic membrane and its characteristic peaks are: $2\theta = 25.46^\circ, 35.06^\circ,$
339 $37.73^\circ, 43.24^\circ, 52.47^\circ, 57.42^\circ, 60.61^\circ, 66.44^\circ, 76.77^\circ, 86.26^\circ$ and 88.83° . Furthermore, the
340 diffraction peaks of SiO_2 ($2\theta = 36.56^\circ, 59.95^\circ, 68.12^\circ, 77.65^\circ, 80.04^\circ$ and 84.95°) are also found in
341 the figure. It is verified that SiO_2 is one of the main components of ceramic membrane. The
342 characteristic peaks of Ni ($2\theta = 44.41^\circ, 51.77^\circ, 76.33^\circ$) are detected which illustrates the presence of
343 Ni in fresh Ni-CM and used E4-Ni-CM. Moreover, it is noticeable that no peaks of NiO appear on
344 the curves. It indicates that Ni on fresh Ni-CM and used Ni-CM exists in the form of active single
345 substance. The deactivation of Ni-CM catalyst is due to the fact that the surface of the Ni-CM
346 catalyst is almost completely covered by carbon during the oily sludge pyrolysis process [33].

347 **4. Conclusion**

348 Ni-ceramic membrane catalyst was prepared by impregnation method and characterized in this study.
349 The clean catalytic pyrolysis of oily sludge was carried out on the spiral reactor to study the effect of
350 ceramic membrane on oily sludge pyrolysis and particulate removal. It was found that the Ni loading
351 on the ceramic membrane could improve the yield of the pyrolysis gas. The yield of the pyrolysis gas
352 produced from the reaction with Ni-ceramic membrane was 31.46 L/kg, while the recovery rate of
353 pyrolysis oil was 48.21%. On the contrary, the yield of the pyrolysis gas produced from the reaction
354 with clean ceramic membrane was 17.92 L/kg, while the recovery rate of pyrolysis oil was 62.63%.
355 The results indicate that the ceramic membrane has a great removal effect on solid particles from
356 pyrolysis products. In addition, a long-time catalytic pyrolysis experiment was carried out. With the
357 feeding speed of 4.17 g/min and reaction temperature of 500°C, the Ni-ceramic membrane could be
358 used continuously for 420 min. As a result, Ni-ceramic membrane catalyst can be used for the
359 pyrolysis of oily sludge.

360 **Acknowledgement**

361 This project has received funding from the Key Program for China EU International Cooperation in
362 Science and Technology Innovation (No. 2018YFE0117300), Shaanxi Provincial Natural Science
363 Foundation Research Program-Shaanxi Coal Joint Funding (2019JLZ-12). The Horizon 2020, Marie
364 Curie Research and Innovation Staff Exchange (RISE) (No.823745). And many thanks to the
365 technicians in Analytical and Testing Center of Xi'an Jiaotong University.

366 **References**

367 [1] Zhang J, Li J, Thring RW, Hu X, Song X. Oil recovery from refinery oily sludge via
368 ultrasound and freeze/thaw. *Journal of Hazardous Materials* 2012;203:195-203.

- 369 <https://doi.org/10.1016/j.jhazmat.2011.12.016>.
- 370 [2] Heidarzadeh N, Gitipour S, Abdoli MA. Characterization of oily sludge from a Tehran oil
371 refinery. *Waste Management & Research* 2010;28(10):921-7.
372 <https://doi.org/10.1177/0734242x09345794>.
- 373 [3] Gao N, Li J, Quan C, Tan H. Product property and environmental risk assessment of heavy
374 metals during pyrolysis of oily sludge with fly ash additive. *Fuel* 2020;266.
375 <https://doi.org/10.1016/j.fuel.2020.117090>.
- 376 [4] Hu G, Li J, Zeng G. Recent development in the treatment of oily sludge from petroleum
377 industry: A review. *Journal of Hazardous Materials* 2013;261:470-90.
378 <https://doi.org/10.1016/j.jhazmat.2013.07.069>.
- 379 [5] Zhou X, Jia H, Qu C, Fan D, Wang C. Low-temperature co-pyrolysis behaviours and kinetics
380 of oily sludge: effect of agricultural biomass. *Environmental Technology* 2017;38(3):361-9.
381 <https://doi.org/10.1080/09593330.2016.1194481>.
- 382 [6] Shen Y, Chen X, Wang J, Ge X, Chen M. Oil sludge recycling by ash-catalyzed
383 pyrolysis-reforming processes. *Fuel* 2016;182:871-8.
384 <https://doi.org/10.1016/j.fuel.2016.05.102>.
- 385 [7] Qin L, Han J, He X, Zhan Y, Yu F. Recovery of energy and iron from oily sludge pyrolysis in
386 a fluidized bed reactor. *Journal of Environmental Management* 2015;154:177-82.
387 <https://doi.org/10.1016/j.jenvman.2015.02.030>.
- 388 [8] Schmidt H, Kaminsky W. Pyrolysis of oil sludge in a fluidised bed reactor. *Chemosphere*
389 2001;45(3):285-90. [https://doi.org/10.1016/s0045-6535\(00\)00542-7](https://doi.org/10.1016/s0045-6535(00)00542-7).
- 390 [9] Silva DC, Silva AA, Melo CF, Marques MRC. Production of oil with potential energetic use

- 391 by catalytic co-pyrolysis of oil sludge from offshore petroleum industry. *J Anal Appl*
392 *Pyrolysis* 2017;124:290-7. <https://doi.org/10.1016/j.jaap.2017.01.021>.
- 393 [10] Cheng S, Wang Y, Fumitake T, Kouji T, Li A, Kunio Y. Effect of steam and oil sludge ash
394 additive on the products of oil sludge pyrolysis. *Applied Energy* 2017;185:146-57.
395 <https://doi.org/10.1016/j.apenergy.2016.10.055>.
- 396 [11] Lin B, Wang J, Huang Q, Chi Y. Effects of potassium hydroxide on the catalytic pyrolysis of
397 oily sludge for high-quality oil product. *Fuel* 2017;200:124-33.
398 <https://doi.org/10.1016/j.fuel.2017.03.065>.
- 399 [12] Panek P, Kostura B, Cepelakova I, Koutnik I, Tomsej T. Pyrolysis of oil sludge with
400 calcium-containing additive. *J Anal Appl Pyrolysis* 2014;108:274-83.
401 <https://doi.org/10.1016/j.jaap.2014.04.005>.
- 402 [13] Izhar S, Uehara S, Yoshida N, Yamamoto Y, Morioka T, Nagai M. Hydrodenitrogenation of
403 fast pyrolysis bio-oil derived from sewage sludge on NiMo/Al₂O₃ sulfide catalyst. *Fuel*
404 *Process Technol* 2012;101:10-5. <https://doi.org/10.1016/j.fuproc.2012.03.012>.
- 405 [14] Shie JL, Chang CY, Lin JP, Lee DJ, Wu CH. Use of inexpensive additives in pyrolysis of oil
406 sludge. *Energy & Fuels* 2002;16(1):102-8. <https://doi.org/10.1021/ef0100810>.
- 407 [15] Song Q, Zhao H, Jia J, Zhang F, Wang Z, Lv W, et al. Characterization of the products
408 obtained by pyrolysis of oil sludge with steel slag in a continuous pyrolysis-magnetic
409 separation reactor. *Fuel* 2019;255. <https://doi.org/10.1016/j.fuel.2019.115711>.
- 410 [16] Rezaei M, Alavi SM, Sahebdehfar S, Yan Z-F. Nanocrystalline zirconia as support for nickel
411 catalyst in methane reforming with CO₂. *Energy & Fuels* 2006;20(3):923-9.
412 <https://doi.org/10.1021/ef050384k>.

- 413 [17] Hegarty MES, O'Connor AM, Ross JRH. Syngas production from natural gas using
414 ZrO₂-supported metals. *Catalysis Today* 1998;42(3):225-32.
415 [https://doi.org/10.1016/s0920-5861\(98\)00096-0](https://doi.org/10.1016/s0920-5861(98)00096-0).
- 416 [18] Chai Y, Gao N, Wang M, Wu C. H₂ production from co-pyrolysis/gasification of waste
417 plastics and biomass under novel catalyst Ni-CaO-C. *Chem Eng J* 2020;382.
418 <https://doi.org/10.1016/j.cej.2019.122947>.
- 419 [19] Wang SB, Lu GQ. Reforming of methane with carbon dioxide over Ni/Al₂O₃ catalysts: Effect
420 of nickel precursor. *Applied Catalysis a-General* 1998;169(2):271-80.
421 [https://doi.org/10.1016/s0926-860x\(98\)00017-9](https://doi.org/10.1016/s0926-860x(98)00017-9).
- 422 [20] Quan C, Gao N, Wang H, Sun H, Wu C, Wang X, et al. Ethanol steam reforming on Ni/CaO
423 catalysts for coproduction of hydrogen and carbon nanotubes. *International Journal of Energy*
424 *Research* 2019;43(3):1255-71. <https://doi.org/10.1002/er.4365>.
- 425 [21] Barredo-Damas S, Alcaina-Miranda MI, Bes-Pia A, Iborra-Clar MI, Iborra-Clar A,
426 Mendoza-Roca JA. Ceramic membrane behavior in textile wastewater ultrafiltration.
427 *Desalination* 2010;250(2):623-8. <https://doi.org/10.1016/j.desal.2009.09.037>.
- 428 [22] Simeone E, Nacken M, Haag W, Heidenreich S, de Jong W. Filtration performance at high
429 temperatures and analysis of ceramic filter elements during biomass gasification. *Biomass &*
430 *Bioenergy* 2011;35:S87-S104. <https://doi.org/10.1016/j.biombioe.2011.04.036>.
- 431 [23] Gao N, Wang X, Quan C, Wu C. Study of oily sludge pyrolysis combined with fine particle
432 removal using a ceramic membrane in a fixed-bed reactor. *Chemical Engineering and*
433 *Processing-Process Intensification* 2018;128:276-81.
434 <https://doi.org/10.1016/j.cep.2018.03.002>.

- 435 [24] Ma Z, Xie J, Gao N, Quan C. Pyrolysis behaviors of oilfield sludge based on Py-GC/MS and
436 DAEM kinetics analysis. *Journal of the Energy Institute* 2019;92(4):1053-63.
437 <https://doi.org/10.1016/j.joei.2018.07.001>.
- 438 [25] Chang CY, Shie JL, Lin JP, Wu CH, Lee DJ, Chang CF. Major products obtained from the
439 pyrolysis of oil sludge. *Energy & Fuels* 2000;14(6):1176-83.
440 <https://doi.org/10.1021/ef0000532>.
- 441 [26] Vamvuka D, Salpigidou N, Kastanaki E, Sfakiotakis S. Possibility of using paper sludge in
442 co-firing applications. *Fuel* 2009;88(4):637-43. <https://doi.org/10.1016/j.fuel.2008.09.029>.
- 443 [27] Gao N, Han Y, Quan C. Study on steam reforming of coal tar over Ni-Co/ceramic foam
444 catalyst for hydrogen production: Effect of Ni/Co ratio. *International Journal of Hydrogen
445 Energy* 2018;43(49):22170-86. <https://doi.org/10.1016/j.ijhydene.2018.10.119>.
- 446 [28] Gao N, Liu S, Han Y, Xing C, Li A. Steam reforming of biomass tar for hydrogen production
447 over NiO/ceramic foam catalyst. *Int J Hydrogen Energy* 2015;40(25):7983-90.
448 <https://doi.org/10.1016/j.ijhydene.2015.04.050>.
- 449 [29] Simeone E, Siedlecki M, Nacken M, Heidenreich S, de Jong W. High temperature gas
450 filtration with ceramic candles and ashes characterisation during steam-oxygen blown
451 gasification of biomass. *Fuel* 2013;108:99-111. <https://doi.org/10.1016/j.fuel.2011.10.030>.
- 452 [30] Kan T, Xiong J, Li X, Ye T, Yuan L, Torimoto Y, et al. High efficient production of hydrogen
453 from crude bio-oil via an integrative process between gasification and current-enhanced
454 catalytic steam reforming. *Int J Hydrogen Energy* 2010;35(2):518-32.
455 <https://doi.org/10.1016/j.ijhydene.2009.11.010>.
- 456 [31] Meesuk S, Cao J-P, Sato K, Ogawa Y, Takarada T. Study of Catalytic Hydrolysis of Rice

- 457 Husk under Nickel-Loaded Brown Coal Char. *Energy & Fuels* 2011;25(11):5438-43.
458 <https://doi.org/10.1021/ef201266b>.
- 459 [32] D'Orazio A, Rapagna S, Foscolo PU, Gallucci K, Nacken M, Heidenreich S, et al. Gas
460 conditioning in H₂ rich syngas production by biomass steam gasification: Experimental
461 comparison between three innovative ceramic filter candles. *Int J Hydrogen Energy*
462 2015;40(23):7282-90. <https://doi.org/10.1016/j.ijhydene.2015.03.169>.
- 463 [33] Wu C, Williams PT. Hydrogen production by steam gasification of polypropylene with
464 various nickel catalysts. *Applied Catalysis B-Environmental* 2009;87(3-4):152-61.
465 <https://doi.org/10.1016/j.apcatb.2008.09.003>.
- 466